

# Facet modulation selective epitaxy—a technique for quantum-well wire doublet fabrication

Charles S. Tsai, John A. Lebens, Channing C. Ahn,<sup>a)</sup> Akbar Nouhi,<sup>b)</sup> and Kerry J. Vahala  
*Department of Applied Physics, Mail Stop 128-95, California Institute of Technology, Pasadena, California 91125*

(Received 26 September 1991; accepted for publication 11 November 1991)

The technique of facet modulation selective epitaxy and its application to quantum-well wire doublet fabrication are described. Successful fabrication of wire doublets in the  $\text{Al}_x\text{Ga}_{1-x}\text{As}$  material system is achieved. The smallest wire fabricated has a crescent cross section less than 140 Å thick and less than 1400 Å wide. Backscattered electron images, transmission electron micrographs, cathodoluminescence spectra, and spectrally resolved cathodoluminescence images of the wire doublets are presented.

Semiconductor structures exhibiting quantum confinement in two or three dimensions have attracted considerable attention for their potential in improving optoelectronic devices<sup>1,2</sup> and in revealing new phenomena in solid-state physics, such as polarization anisotropy in quantum wires.<sup>3</sup> Many approaches to fabricate these quantum-confined structures have been studied. Already grown quantum-well material has been physically patterned by a combination of lithography and etching<sup>4-6</sup> or has been selectively disordered by ion implantation<sup>7</sup> to achieve lateral confinement. *In situ* formation of nanostructures during epitaxial growths has also been studied. Migration-enhanced epitaxy on tilted substrates has exhibited quantum-confinement effects,<sup>8</sup> and stimulated emission from quantum wires<sup>9</sup> has been demonstrated by performing metalorganic vapor-phase epitaxy (MOVPE) growths on etched substrates. Recently, wire and dot structures have been selectively grown on substrates covered with patterned dielectric masks.<sup>10-12</sup> The formation of crystal facets in single precursor chemistry (trimethyl) selective growth has also been studied as a potential method for quantum-well wire fabrication.<sup>13</sup>

In this letter, we describe a new technique, facet modulation selective epitaxy, and present its application to quantum-well wire doublet fabrication in the  $\text{Al}_x\text{Ga}_{1-x}\text{As}$  material system. Facet modulation selective epitaxy, as it is defined here, is the application of different precursor chemistries to layers within a single growth to alter sequentially the appearance of facets on a growing structure and to thereby form heterostructures of novel geometry. Two precursor chemistries are used here: a combination of diethylgallium chloride (DEGaCl) and arsine ( $\text{AsH}_3$ ) for GaAs growth and a combination of trimethylaluminum (TMAI), trimethylgallium (TMGa), and arsine ( $\text{AsH}_3$ ) for  $\text{Al}_x\text{Ga}_{1-x}\text{As}$  growth. The morphology of GaAs selective growth using DEGaCl and  $\text{AsH}_3$  is dominated by the appearance of the {111} and {110} families of slow growth planes, with the appearance of a particular plane dependent

on the growth temperature and the mask opening orientation.<sup>10,11,14</sup> The morphology of  $\text{Al}_x\text{Ga}_{1-x}\text{As}$  selective growth using TMAI, TMGa, and  $\text{AsH}_3$  is similar, but the bounding planes include higher-index-number planes (one or more indices greater than one) in addition to the {111} and {110} families of slow growth planes.

One application of facet modulation selective epitaxy is the fabrication of quantum-well wire doublets in one single growth as illustrated in Fig. 1. Using DEGaCl and  $\text{AsH}_3$ , a GaAs buffer bounded by the low-index-number facets is grown on a substrate covered with a stripe patterned mask, then an  $\text{Al}_x\text{Ga}_{1-x}\text{As}$  layer is grown using TMAI, TMGa, and  $\text{AsH}_3$ . Using DEGaCl and  $\text{AsH}_3$  again, a GaAs wire doublet is formed as the higher-index-number  $\text{Al}_x\text{Ga}_{1-x}\text{As}$  facets are partially filled by the GaAs growth attempting to form low-index-number GaAs facets. The wire doublet is buried *in situ* by another layer of  $\text{Al}_x\text{Ga}_{1-x}\text{As}$  growth to eliminate any free surface that would produce nonradiative recombination centers. The width of the starting  $\text{Al}_x\text{Ga}_{1-x}\text{As}$  facets and the amount of GaAs deposited determine the size of the wires and the spacing between wires in a wire doublet. In the work presented here, successful fabrication of wire doublets by facet modulation selective epitaxy is achieved. Analysis of these

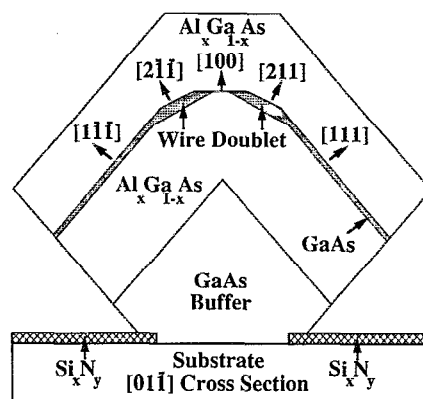


FIG. 1. Schematic illustration of quantum-well wire doublet fabrication by facet modulation selective epitaxy.

<sup>a)</sup>Present address: Department of Materials Science, Mail Stop 138-78, California Institute of Technology, Pasadena, CA 91125.

<sup>b)</sup>Present address: Department of Electrical Engineering, California State Polytechnic University, Pomona, CA 91768.

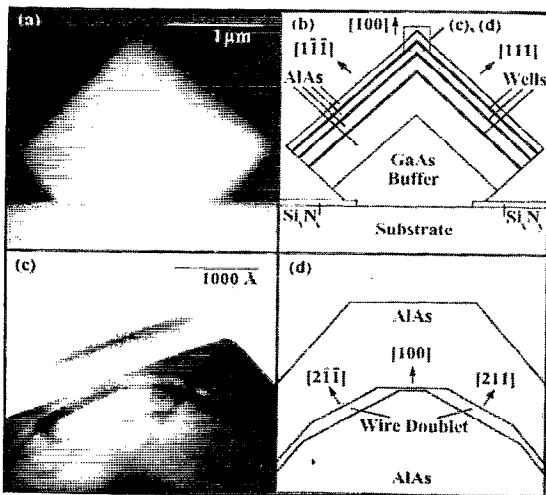


FIG. 2. (a)  $[01\bar{1}]$  cross-sectional backscattered electron image of a complete structure grown by facet modulation selective epitaxy. (b) Schematic illustration of the complete structure. (c)  $[01\bar{1}]$  cross-sectional transmission electron micrograph of the wire doublet. (d) Schematic illustration of the wire doublet.

wire doublet structures by backscattered electron microscopy, transmission electron microscopy, and cathodoluminescence scanning electron microscopy is presented.

The substrates used in this study contained a  $2\text{-}\mu\text{m}$  Si-doped  $\text{Al}_{0.4}\text{Ga}_{0.6}\text{As}$  layer, an undoped  $100\text{-nm}$   $\text{Al}_{0.2}\text{Ga}_{0.8}\text{As}$  layer, and a  $10\text{-nm}$  GaAs cap layer all deposited by MOVPE on Si-doped (100) GaAs substrates. The dielectric mask was  $175\text{ \AA}$  of silicon nitride deposited by plasma-enhanced chemical vapor deposition. Arrays of  $5\text{-mm}$ -long stripe openings, with stripe widths varying from  $1$  to  $8\text{ }\mu\text{m}$  and center-to-center spacing between stripes of  $250\text{ }\mu\text{m}$ , were patterned into the silicon nitride mask by photolithography and reactive-ion etching in  $\text{CF}_4$  plasma. The stripes were oriented along the  $[01\bar{1}]$  direction.

Sample growth was performed in an atmospheric-pressure MOVPE reactor with graphite susceptor temperature set to  $730\text{ }^\circ\text{C}$ . Precursors for the buffer and the wells were  $\text{DEGaCl}$  and  $\text{AsH}_3$ . Precursors for the barriers were  $\text{TMAI}$  and  $\text{AsH}_3$ . AlAs barriers were chosen here to test the extreme case. Growth interruptions were placed between layers while  $\text{AsH}_3$  flow was maintained. No dopant was intentionally introduced.

Figures 2(a) and 2(b) show a complete structure grown in a stripe opening  $1.2\text{ }\mu\text{m}$  wide. The structure exhibits a faceted profile bounded mainly by the  $\{111\}$  family of planes. Measured along the  $[100]$  crystal direction from the substrate to the crystal vertex, the growth consists of  $1.3\text{ }\mu\text{m}$  of GaAs,  $0.6\text{ }\mu\text{m}$  of AlAs, first well,  $0.4\text{ }\mu\text{m}$  of AlAs, second well,  $0.2\text{ }\mu\text{m}$  of AlAs, third well, and finally  $0.13\text{ }\mu\text{m}$  of AlAs. Measured along the  $[111]$  crystal direction on the  $(111)$  facet, the first, second, and third wells are approximately  $10$ ,  $20$ , and  $5\text{ nm}$  thick, respectively.

The wire doublet is shown clearly in Figs. 2(c) and 2(d). The transmission electron micrograph in Fig. 2(c) reveals the higher-index-number  $\{211\}$ -type AlAs facets near the crystal vertex. The micrograph also shows the

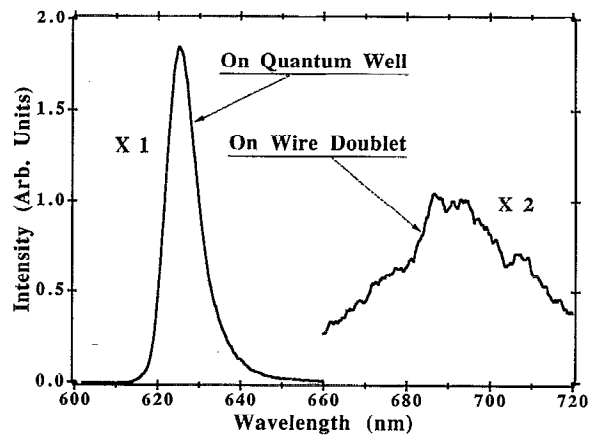


FIG. 3. Cathodoluminescence spectra of the region near the wire doublet. The sample is at  $14\text{ K}$ .

third-well growth partially filling in the two  $\{211\}$ -type facets, thereby forming a wire doublet as predicted earlier. The two wires in the wire doublet are almost identical in shape and size. Both wires are approximately  $140\text{ \AA}$  thick at the center and  $1400\text{ \AA}$  wide, although the effective width of these wires is probably smaller than  $1400\text{ \AA}$ , because the wires have a tapered cross section.

The luminescence properties of these wire doublet structures were investigated by applying low-temperature cathodoluminescence (CL) scanning electron microscopy.<sup>15</sup> Figure 3 contains the CL spectra of the sample region near the wire doublet. Two distinct peaks appear in the CL spectra: one from the wire doublet at  $690\text{ nm}$  and another from the side-wall quantum wells at  $625\text{ nm}$ . The red shifting of the wire doublet peak with respect to the side-wall quantum-well peak is as expected from the thickness modulation illustrated in Fig. 2(c). However, it is clear from the CL spectra and the thicknesses measured from Fig. 2(c) that the wire doublet and the side-wall quantum wells are most likely  $\text{Al}_{0.2}\text{Ga}_{0.8}\text{As}$ , not GaAs, because a  $140\text{-}\text{\AA}$  GaAs quantum well at  $14\text{ K}$  luminesces at about  $800\text{ nm}$ , not at  $690\text{ nm}$  as in the CL spectra, and a  $50\text{-}\text{\AA}$  well luminesces at about  $710\text{ nm}$ , not at  $625\text{ nm}$ . Here the wire doublet is approximated as a quantum well because the widths of the wires are much larger than their thicknesses. The presence of aluminum is due to interlayer mixing, presumably caused by incomplete purging of TMAI before the  $\text{DEGaCl}$  growth had begun. The wire doublet luminescence peak at  $690\text{ nm}$  also appears broadened. Possible reasons for this broadening may include the fluctuations in the width of the  $\{211\}$ -type AlAs facets, the surface roughness on the  $\{211\}$ -type AlAs facets, or some aluminum segregation from mixing the two precursor chemistries.

Figures 4(a)–4(c) are spectrally resolved CL images of the wire doublet structure in cross section. Figure 4(a) is imaged at  $625\text{ nm}$  where the side-wall quantum wells and the substrate  $\text{Al}_{0.4}\text{Ga}_{0.6}\text{As}$  luminesce. Figure 4(b) is imaged at  $693\text{ nm}$ , the luminescence peak of the wire doublet. Figure 4(c) is imaged at  $820\text{ nm}$ , the luminescence

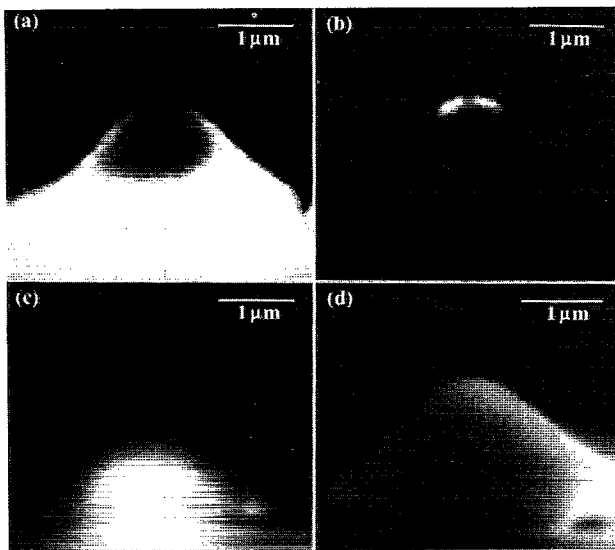


FIG. 4. Spectrally resolved cathodoluminescence images of a wire doublet structure in cross section. The sample is at 12 K, and the wavelengths are set at (a) 625 nm, (b) 693 nm, and (c) 820 nm. (d) Scanning electron micrograph of the same structure in cross section.

wavelength of the buffer and substrate GaAs. The scanning electron micrograph in Fig. 4(d) shows the cross section imaged in Figs. 4(a)–4(c). Figures 5(a)–5(d) are spectrally resolved CL images of structures seeded by different stripe opening widths on the same sample. These images

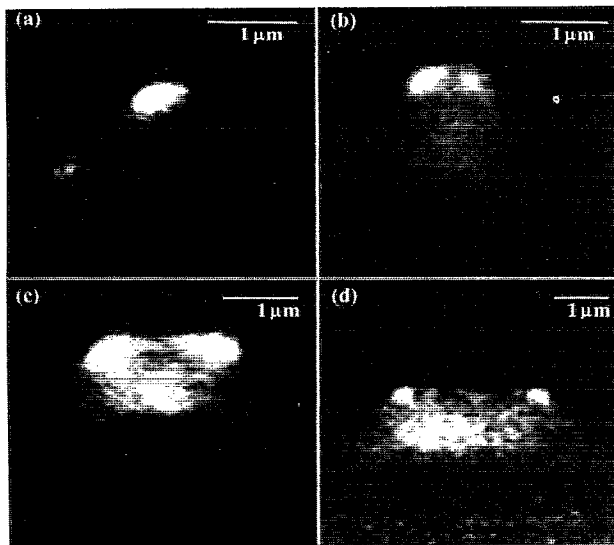


FIG. 5. Spectrally resolved cathodoluminescence images of different wire doublet structures on the same sample. The sample is at 77 K, and the wavelengths are set at (a)–(c) 690 nm and (d) 680 nm.

demonstrate the various wire doublet configurations.

In conclusion, the technique of facet modulation selective epitaxy and its application to quantum-well wire doublet fabrication have been described. Successful fabrication of wire doublets in the  $\text{Al}_x\text{Ga}_{1-x}\text{As}$  material system has been achieved. The smallest wire fabricated has a crescent cross section less than 140 Å thick and less than 1400 Å wide. Further reduction in wire size will be pursued by reducing the width of the starting  $\text{Al}_x\text{Ga}_{1-x}\text{As}$  facets and the amount of GaAs deposited. By doping the layers above and below the wire doublet  $p$  and  $n$  type, respectively, and by embedding the wire doublet in an  $\text{Al}_x\text{Ga}_{1-x}\text{As}$  optical waveguide, an injection laser may be fabricated. Other applications will also be explored, including the fabrication of quantum dots and the extensions of this technique to other material systems besides  $\text{Al}_x\text{Ga}_{1-x}\text{As}$ , such as  $\text{In}_x\text{Ga}_{1-x}\text{As}$ , by using analogous precursor chemistries.<sup>11</sup>

This work was supported by grants from the Office of Naval Research (N00014-90-J-1854), DARPA, and the Caltech President's Fund. The authors would like to acknowledge Edward Leigh-Wood and John H. Coleman of the Plasma Physics Corp., New York, for the dielectric mask deposition, and Robert J. Lang and Barbara A. Wilson of the NASA Jet Propulsion Laboratory for assistance in using the MOVPE reactor. The transmission electron microscopy work was supported by a grant from the National Science Foundation (DMR-8811795). C. S. T. would like to acknowledge the support of a National Science Foundation graduate fellowship.

- <sup>1</sup>Y. Arakawa, K. Vahala, and A. Yariv, *Appl. Phys. Lett.* **45**, 950 (1984).
- <sup>2</sup>M. Asada, Y. Miyamoto, and Y. Suematsu, *IEEE J. Quantum Electron.* **QE-22**, 1915 (1986).
- <sup>3</sup>P. C. Sercel and K. J. Vahala, *Appl. Phys. Lett.* **57**, 545 (1990).
- <sup>4</sup>K. Kash, A. Scherer, J. M. Worlock, H. G. Craighead, and M. C. Tamargo, *Appl. Phys. Lett.* **49**, 1043 (1986).
- <sup>5</sup>H. Temkin, G. J. Dolan, M. B. Panish, and S. N. G. Chu, *Appl. Phys. Lett.* **50**, 413 (1987).
- <sup>6</sup>B. I. Miller, A. Shahar, U. Koren, and P. J. Corvini, *Appl. Phys. Lett.* **54**, 188 (1989).
- <sup>7</sup>J. Cibert, P. M. Petroff, G. J. Dolan, S. J. Pearton, A. C. Gossard, and J. H. English, *Appl. Phys. Lett.* **49**, 1275 (1986).
- <sup>8</sup>M. Tsuchiya, J. M. Gains, R. H. Yan, R. J. Simes, P. O. Holtz, L. A. Coldren, and P. M. Petroff, *Phys. Rev. Lett.* **62**, 466 (1989).
- <sup>9</sup>E. Kapon, D. M. Hwang, and R. Bhat, *Phys. Rev. Lett.* **63**, 430 (1989).
- <sup>10</sup>J. A. Lebens, C. S. Tsai, K. J. Vahala, and T. F. Kuech, *Appl. Phys. Lett.* **56**, 2642 (1990).
- <sup>11</sup>T. F. Kuech, M. S. Goorsky, M. A. Tischler, A. Palevski, P. Solomon, R. Potemski, C. S. Tsai, J. A. Lebens, and K. J. Vahala, *J. Cryst. Growth* **107**, 116 (1991).
- <sup>12</sup>Y. D. Galeuchet, H. Rothuizen, and P. Roentgen, *Appl. Phys. Lett.* **58**, 2423 (1991).
- <sup>13</sup>S. Ando and T. Fukui, *J. Cryst. Growth* **98**, 646 (1989).
- <sup>14</sup>T. F. Kuech, M. A. Tischler, and R. Potemski, *Appl. Phys. Lett.* **54**, 910 (1989).
- <sup>15</sup>M. E. Hoenk and K. J. Vahala, *Rev. Sci. Instrum.* **60**, 226 (1989).